Apoptosis (2019) 24:562–577
https://doi.org/10.1007/s10495-019-01539-7

Recombinant human lactoferrin induces apoptosis, disruption of F-actin structure and cell cycle arrest with selective cytotoxicity on human triple negative breast cancer cells

Blanca F. Iglesias-Figueroa[1] · Tania S. Siqueiros-Cendón[1] · Denisse A. Gutierrez[2] · Renato J. Aguilera[2] · Edward A. Espinoza-Sánchez[1] · Sigifredo Arévalo-Gallegos[1] · Armando Varela-Ramirez[2] · Quintín Rascón-Cruz[1]

Published online: 2 April 2019

Abstract

Breast cancer is the most frequently diagnosed cancer among women worldwide. Here, recombinant human lactoferrin (rhLf) expressed in *Pichia pastoris* was tested for its potential cytotoxic activity on a panel of six human breast cancer cell lines. The rhLf cytotoxic effect was determined via a live-cell HTS imaging assay. Also, confocal microscopy and flow cytometry protocols were employed to investigate the rhLf mode of action. The rhLf revealed an effective CC_{50} of 91.4 and 109.46 µg/ml on non-metastatic and metastatic MDA-MB-231 cells, with favorable selective cytotoxicity index values, 11.68 and 13.99, respectively. Moreover, rhLf displayed satisfactory SCI values on four additional cell lines, MDA-MB-468, HCC70, MCF-7 and T-47D (1.55–3.34). Also, rhLf provoked plasma membrane blebbing, chromatin condensation and cell shrinkage in MDA-MB-231 cells, being all three apoptosis-related morphological changes. Also, rhLf was able to shrink the microfilaments, forming a punctuated cytoplasmic pattern in both the MDA-MB-231 and Hs-27 cells, as visualized in confocal photomicrographs. Moreover, performing flow cytometric analysis, rhLf provoked significant phosphatidylserine externalization, cell cycle arrest in the S phase and apoptosis-induced DNA fragmentation in MDA-MB-231 cells. Hence, rhLf possesses selective cytotoxicity on breast cancer cells. Also, rhLf caused apoptosis-associated morphologic changes, disruption of F-actin cytoskeleton organization, phosphatidylserine externalization, DNA fragmentation, and arrest of the cell cycle progression on triple-negative breast cancer MDA-MB-231 cells. Overall results suggest that rhLf is using the apoptosis pathway as its mechanism to inflict cell death. Findings warranty further evaluation of rhLf as a potential anti-breast cancer drug option.

Keywords Lactoferrin · Cytoskeleton · Anti-cancer drug discovery · Apoptosis · Cancer · Cell cycle

Introduction

Lactoferrin (Lf), an iron-binding monomeric glycoprotein, is one of the components of the innate immune system in mammals [1]. Lf is present in almost all body fluids, containing its maximum concentration in colostrum (up to 7 mg/ml) and milk (2 mg/ml) [2]. Considered as a nutraceutical protein [3], the free Lf found in human serum, tears, semen, saliva and other secretions [4], possess immunomodulatory, antimicrobial, antioxidant and anticarcinogenic activities [5]. Lf (formerly known as lactotransferrin) is a well-conserved glycoprotein of around 80 kDa with approximately 700 amino acid residues. However, its length varies in amino acid number according to different species; human Lf is comprised of a 711 amino acids peptide [6].

✉ Armando Varela-Ramirez
avarela2@utep.edu

✉ Quintín Rascón-Cruz
qrascon@uach.mx

[1] Laboratorio de Biotecnología I, Facultad de Ciencias Químicas, Universidad Autónoma de Chihuahua, Circuito Universitarios s/n Nuevo Campus Universitario, C. P. 31125 Chihuahua, Mexico

[2] The Cytometry, Screening and Imaging Core Facility, Border Biomedical Research Center, Department of Biological Sciences, The University of Texas at El Paso, 500 West University Avenue, El Paso, TX 79968-0519, USA

Cancer is the second leading cause of death worldwide, which was just surpassed by heart disease [7]. Globally, approximately one in six deaths is due to cancer [7]. In January 2016, more than 15.5 million Americans were alive with a history of cancer [8]. In the US, around 1,735,350 new cancer cases are predicted to be diagnosed in 2018 [8]. Also, approximately 609,640 Americans are anticipated to die of cancer in 2018, which translates to a rate of 1670 deaths per day [8]. Breast cancer is the most commonly diagnosed cancer in women worldwide [7]. In the US, about 268,670 new cases of breast cancer are expected to be detected for 2018; 266,120 women and 2550 men. In addition, it is predicted that 41,400 deaths (40,920 women and 480 men) from breast cancer will occur during 2018 in the US [8]. In the US, around 1,762,450 new cancer cases are predicted to be diagnosed in 2019 [8]. Also, approximately 606,880 Americans are anticipated to die of cancer in 2019, which translates to a rate of 1662 deaths per day [8]. Breast cancer is the most commonly diagnosed cancer in women worldwide [7]. In the US, about 271,270 new cases of breast cancer are expected to be detected for 2019; 268,600 women and 2670 men. In addition, it is predicted that 42,260 deaths (41,760 women and 500 men) from breast cancer will occur during 2019 in the US [8]. Currently, oncological treatments may involve radiation, chemotherapy and/or surgeries, which implies severe physiological and psychological damage for patients undergoing such procedures. With all those alarming numbers and the undesired secondary effect provoked by the presently available anticancer therapies, it is therefore imperative to identify and validate novel effective experimental compounds with anticancer activity and furthermore, with anti-breast cancer effects.

In line with the above context, Lf has been studied for its anticarcinogenic effect [9, 10]. It has been shown that Lf exerts cytotoxic activity on various cancer cells, and also, the bioactive lactoferrin-derived peptides were able to induce programmed cell death in cancer cells [11]. Moreover, it has been shown that Lf induced a disruptive effect in the cell cycle profile, being able to arrest cells at different facets of the cell cycle, depending on the cancer cell type studied [12]. On the other hand, Lf is a molecule capable of chelating iron ions, transfer iron to cells and also has an anticancer activity based on its ability to balance this ion in the blood and external secretions [13]. Previously, it was demonstrated that tumor cells demanded higher concentrations of iron to grow and also, the genes implicated in iron uptake were highly over-expressed in tumor cells [14]. Therefore, Lf could be additionally implicated in the mechanisms of cancer drug resistance related to iron metabolism [15], and also, on induction of ferroptosis, an iron-related cell death mechanism [16, 17].

In the present study, recombinant human lactoferrin (rhLf) expressed in the yeast *Pichia pastoris*, exerted a selective cytotoxic effect on human triple negative breast cancer cells, with minimum damage on non-cancerous breast cells. Also, results suggest that rhLf used the apoptotic pathway as a mechanism to inflict its cytotoxic activity, as evidenced by provoking cellular morphological changes associated with apoptosis, such as; disruption of the F-actin microfilaments, externalization of phosphatidylserine, apoptosis-induced DNA fragmentation, and alteration of the normal cell cycle progression. With these findings, the panorama of possibilities for the generation of new natural pharmacological alternatives in cancer patients is opened.

Materials and methods

Enzymes, strains, and culture conditions

All restriction enzymes were purchased from Invitrogen® (Carlsbad, CA, USA). *Escherichia coli* (*E. coli*) BL21DE3 (Invitrogen®) was used as a host for plasmid propagation. *Pichia pastoris* (*P. pastoris*) X33 (provided by CIAD, Cd. Cuauhtémoc, Chih. Mexico) was used for protein expression. *E. coli* BL21DE3 was cultured at 37 °C in Luria–Bertani (LB) broth (10 mg/L tryptone, 5 mg/L yeast extract, 10 mg/L NaCl) and LB plates (15 mg/mL agar) supplemented with zeocin (25 µg/mL) as the selective marker. *P. pastoris* was cultured at 30 °C and 250 rpm on YPD (1% yeast extract, 2% peptone, 2% dextrose) broth and YPD plates (20 mg/mL agar) supplemented with zeocin (200 mg/L) as the selective marker.

Cloning of the human lactoferrin (HLF1) gene and *P. pastoris* transformation

The HLF1 gene is comprised of an open reading frame (ORF) of 2331 bp in size, encoding for 711 amino acids polypeptide with a predicted molecular weight of 78.4 kDa and an estimated PI of 8.12 (Protein calculator v3.4 http://protcalc.sourceforge.net/cgi-bin/protcalc). The human lactoferrin gene (GeneBank accession number M83202.1; isolated from mammary gland tissue of 8 months pregnant female adult) was modified *in silico*, using SnapGene® 4.1.9 software, to optimize the codon usage in *P. pastoris*; also, silent point mutations were made to eliminate undesirable restriction sites, and the six-histidine tag was added at the carboxyl terminus of the sequence. *In silico* modified human lactoferrin sequence was sent to GenScript® (Piscataway, NJ, USA) to be cloned into pPICZα vector (Invitrogen®) and give rise to pIGF5 (Iglesias-Figueroa-IGF) genetic construct. The genetic construction was transformed into *E. coli* BL21DE3 competent cells, and six putative clones were verified by DNA enzymatic restriction analysis. After characterization, one selected clone was linearized with

*Sac*I, and 500 ng of linearized DNA was used to transform *P. pastoris* X33 electrocompetent cells. The transformation was achieved using a MicroPulser BioRad (BioRad, Hercules, CA, USA) according to the manufacturer's instructions. After 3 days of incubation in the presence of the selective marker (200 mg/L zeocine), zeocin-resistant clones were isolated for analysis.

Molecular analyses and rhLf protein induction expression

Pichia pastoris colonies carrying the plasmid of interest were selected on the basis of their zeocin-resistance marker. Additionality, to confirm the presence of the hLf gene in the zeocin-resistance selected colonies, single colony PCR was performed. A yeast colony surpassing the two selection requisites was grown in YPD (10% yeast extract, 20% peptone and 20% D-glucose) broth containing 200 mg/mL zeocine at 30 °C at 250 rpm for 24 h. Then, the cells were harvested by centrifugation and incubated at a seeding density of 0.1–0.2 optical density (OD) in BMMY medium [100 mM potassium phosphate, pH 6.0, 1% yeast extract, 2% peptone, 1.3% yeast nitrogen base (YNB), 400 µg/L biotin and 0.5% methanol] to induce the expression of rhLf. Methanol was again added to a final concentration of 0.5% (v/v) every 24 h for 96 h to maintain the induction according to the method described in [18]. After 96 h, the cells were harvested by centrifugation at 5000 rpm for 10 min at 4 °C, and the culture medium supernatant was collected and tested for the presence of the rhLf secretion using 12% SDS-PAGE.

Protein purification and western blot analysis

The yeast culture supernatant was dialyzed against PBS pH 7.4 for 24 h. After dialysis, the protein extracts were purified using a high-affinity Ni-Charged Resin (GenScript®) according to the manufacturer's instructions to obtain purified rhLf protein. The content of endotoxin levels in the purified rhLf was measured with ToxinSensor TM Chromogenic LAL Endotoxin Assay Kit (GenScript®) which can detect until 0.25 EU/mL according to the manufacturer's instructions. Purified rhLf was boiled with 1 × loading buffer sample for 5 min and separated by SDS-PAGE using 12% resolving and 5% staking acrylamide gel. Separated proteins via electrophoresis were stained with Coomassie Brilliant Blue R-250 to determine protein expression levels. Pre-stained protein marker for western blot analysis (20–250 kDa, Invitrogen) was used as molecular weight standards. After electrophoresis, the separated proteins were transferred from the gels onto a polyvinylidene fluoride (PVDF) microporous membrane (Pierce, Rockford, IL, USA) and blocked overnight at 4 °C using 5% (w/v) bovine serum albumin (BSA) dissolved in Tris-buffered saline (TBS). The blot was then incubated overnight at 4 °C with primary antibody anti-6X His tag rabbit polyclonal antibody (Origene Technologies, Inc., Rockville, MD USA) at a dilution of 1:1000 in 5% w/v of skim milk in TBS-T (0.001% Tween) overnight at 4 °C. Unbound antibody was washed away with TBS-T three times for 15 min each, followed by addition of a secondary antibody (polyclonal goat anti-rabbit conjugated to horseradish peroxidase; Thermo Scientific) at a dilution of 1:10,000 in TBS-T and additionally incubated for 1 h at room temperature. Unbound antibodies were again washed away with TBS-T 3 times for 15 min. Subsequently, an ECL substrate (Thermo Scientific) was added, and the membrane was exposed to a chemiluminescent detection system (iBright FL1000 imaging system; Thermo Scientific).

Cell lines and cell culture conditions

All the seven mammalian cells used in this study were derived from human tissues and were obtained from the American Type Culture Collection (ATCC, Manassas, VA), except the MDA-MB-231/LM2-4 that was a generous gift from Professor Giulio Francia at UTEP [19]. The human triple-negative breast cancer-derived MDA-MB-231 [19], its lung metastatic (LM) variant MDA-MB-231/LM2-4 [20], the triple negative breast cancer MDA-MB-468 [21] and human non-cancerous fibroblast Hs27 cell lines were grown in DMEM medium (Corning, Corning, NY) supplemented with 10% heat-inactivated fetal bovine serum (FBS: Corning), 100 U/mL penicillin and 100 µg/mL streptomycin (Life Technologies, Grand Island, NY). The breast cancer MCF-7 cell line [22], positive for estrogen (ER^+), progesterone (PR^+) and glucocorticoid receptors ($GR/NR3C1^+$), were growth as the above four cell lines, with an extra addition of 10 µg/mL of insulin. The triple negative breast cancer HCC70 cells [23] were maintained in RPMI (Thermo Fisher Scientific Inc.) supplemented with 10% FCS and penicillin/streptomycin. The poorly metastatic breast cancer T-47D cells [24], with estrogen and progesterone receptor (ER^+ and PR^+), were cultured as the HCC70 with the addition of 0.2 U/mL of insulin. The human non-tumorigenic epithelial breast-derived MCF-10A cell line [25], used as a control, was cultured in DMEM/F12 medium (Life Technologies) supplemented with 10% FBS, 10 µg/ml recombinant human insulin (Sigma), 20 ng/ml epidermal growth factor (Peprotech, Rocky Hill, NJ, USA), 0.5 µg/ml hydrocortisone (Sigma), 2.5 mM L-glutamine (Life Technologies), 100 U/ml penicillin and 100 µg/ml streptomycin (Life Technologies) as previously described [26]. All breast-derived cancer cell lines were from female donors and used for the cytotoxicity experiments [27], whereas the Hs27 cell line was derived from a male donor, which was used only for the cytoskeleton analysis. Consistently, the growth conditions for all the cells were at 37 °C in a humidified 5% CO_2 atmosphere. Cells

were prepared as previously recommended to guarantee high viability [28].

Differential nuclear staining (DNS) assay to determine rhLf cytotoxicity activity

All breast-derived cancer cell lines (Table 1), growing in a mid-exponential phase (60–70% confluence) were washed with fresh media, to remove debris and floating cells, which correspond mainly to dead cells. Then, adherent (living) cells were detached by addition of 0.25% trypsin solution (Invitrogen, Carlsbad, CA), diluted in serum-free DMEM medium, and incubated for approximately 10 min at 37 °C [29]. After harvested, cells were counted using a Neubauer chamber and seeded into a 96-multi-well tissue culture plates at a density of 10,000 cells in 100 µl/well of complete media, followed by overnight incubation. Next, cells were treated with 5, 10, and 50 µg/ml of rhLf for 24 h. The following controls were concurrently included in this series of experiments: 5% v/v of H_2O treated cells as a solvent control, untreated cells and as a positive control for cytotoxicity, cells treated with 2 mM of H_2O_2. The differential nuclear staining (DNS) assay was utilized to determine the percentages of cell death [26, 28, 30, 31]. Briefly, two fluorescence DNA binding dyes were used: Hoechst 33342 (Invitrogen, Eugene, OR), a cell membrane permeable fluorophore labeling living and dead cells, thus, providing with the total number of cells, and propidium iodide (PI; MP Biomedicals, Solon, OH), a dye just staining cells with compromised plasma membrane, specifying the total number of dead cells. Two hours before of completion the 24 h incubation period, a mixture of Hoechst and PI was added to the cells for staining purposes, reaching a final concentration of 5 µg/ml each dye. Subsequently, images were captured in a live-cell manner directly from each well of the 96-well plates, by using an IN CELL 2000 bioimager system (GE Healthcare, Chicago, IL). Montages (2×2) from four adjacent image fields were acquired per well to acquire suitable numbers of regions of interest (ROIs = cells), utilizing a ×10 objective and from two individual fluorescence channels accordingly; Hoechst (blue; 451 nm) and PI (red; 617 nm) emission signals. Data analysis and image segmentation were accomplished by using the IN Cell Investigator software (GE Healthcare), specifically designed to assist the bioimager system. Next, the rhLf concentration killing 50% of the cell population (cytotoxic concentration 50%; CC_{50}) was calculated via linear interpolation (https://www.johndcook.com/interpolator.html).

Table 1 The 50% cytotoxic concentration (CC_{50}) exhibited by rhLf on a panel of six human cancer and one non-cancerous breast derived cell lines and its selective cytotoxicity index (SCI)

Cell line	CC_{50} (µg/ml)	SCI[a]
MDA-MB-231[b]	109.46	11.68
MDA-MB-231 LM2-4[c]	91.4	13.99
MDA-MB-468[d]	491.8	2.60
HCC70[e]	823.6	1.55
MCF-7[f]	382.2	3.34
T-47D[g]	491.5	2.60
MCF-10A[h]	1279.4	

[a]The selective cytotoxicity index (SCI) was determined as follow: SCI = CC_{50} of non-cancerous cells/CC_{50} of cancer cells, as previously described [20]

[b]Human triple negative breast cancer MDA-MB-231 cell line; non-metastatic

[c]Lung metastatic (LM) variant derived from MDA-MB-231 cells [19]

[d]Human triple negative breast cancer MDA-MB-468 cell line

[e]Human triple negative cancer HCC70 cell line

[f]Human MCF-7 breast cancer cell line with estrogen, progesterone and glucocorticoid receptors

[g]Human breast cancer with progesterone receptor T-47D cell line

[h]Non-cancerous human epithelial MCF-10A cell line from breast tissue origin used as reference to determine the SCI

Analysis of cellular morphological changes induced by rhLf

The MDA-MB-231 cells growing in plates as described above were treated with 50 µg/ml of rhLf and incubated for 24 h. Next, cells were stained as above by using the DNS assay and images were captured in a live-cells mode utilizing a confocal microscope (LSM 700; Zeiss, New York, NY). Also, confocal images from untreated cells were captured for comparison purposes. Three individual images were acquired, brightfield (differential interference contrast, DIC), Hoechst and PI channels by using a Zen 2009 software (Zeiss), a specifically designed program to assist the confocal microscope.

Preparation of microplates to determine the rhLf effect on the cytoskeleton architecture

For this series of experiments, a confocal microscope approach and the human MDA-MB-231 and Hs27 cell lines were utilized. Before to prepare an experimental 96 multi-well plate, cells were processed as described above and seeded at a density of 2500 cells in 100 µl/well of complete media; this time, the 96 multi-well plates were optically clear, tissue culture-treated imaging plates (BD Falcon, Cat No. 353219). Due that a high magnification objective was utilized to capture the images, wells located in the outermost perimeter of the plate were not used. Then, microplates were incubated overnight to promote cell attachment. Next, MDA-MB-231 cells were incubated with 100 µg/ml (CC_{50}) of rhLf for 2 and 4 h, respectively. As a control, human fibroblast Hs27 cells were incubated with 100 µg/ml of rhLf. Controls

included in this series of experiments were as follow: 5 µg/ml cytochalasin D, an inhibitor of the actin polymerization; 1 µM paclitaxel, as tubulin depolymerization inhibitor; 1% v/v DMSO and 5% v/v H_2O as solvent controls; and untreated cells.

Cell fixation and cytoskeleton staining protocol

After terminated the incubation time, without removing the growing media, each well was gently added with 100 µl of freshly prepared 8% of formaldehyde as a fixative solution, reaching a final formaldehyde concentration of 4%, and incubated for 20 min at room temperature. Then, the fixative solution was removed, and each well was added with 200 µl of 0.1% Tween 20 v/v in PBS for washing and permeabilization purposes and incubated for 10 min at room temperature. Two additional washes with the last solution (0.1% Tween 20 in PBS) were made. For blocking purposes, after removing the permeabilizing solution, 200 µl of 5% w/v of bovine serum albumin (BSA; Sigma) dissolved in TBS-T (Tris-buffered saline containing 0.5% v/v of Tween-20) buffer were added per well and incubated for 1 h on a rocker platform or rotating device at room temperature. Then, cells were triple stained with 50 µl of a 0.1% v/v of Tween 20 PBS solution per well, containing 5 µg/ml of DAPI (Invitrogen), 0.165 µM of Alexa Fluor 568-conjugated phalloidin (Invitrogen) and 0.5 µg/ml of Alexa Fluor 488-conjugated anti-α-tubulin monoclonal antibody (clone DM1A; Thermo Fisher Scientific, Rochester, NY) by incubating 1 h at room temperature in the dark on a rocker platform. Thus, labeling nuclei, actin microfilaments (F-actin) and microtubules (polymerized tubulin), respectively. Next, cells were washed three times using 200 µl of the permeabilizing solution as described above; at the end, 200 µl of the permeabilizing solution was left in the well. Then, images were captured in three fluorescence channels (Alexa-488, Alexa-568, and DAPI) by using a confocal microscope (LSM-700; Zeiss) equipped with an EC Plan-Neofluar 40x/1.30 oil DIC objective [32]. If the fluorescence signals were dissipated or photobleached, it was possible to re-stain the cells using the same mixture as above described, obtaining very bright signals again. During the whole process, cells were never dry.

Analysis of the apoptosis/necrosis pathway via annexin V-FITC/PI assay

The MDA-MB-231 cells seeded at a density of 100,000 cells/well in 1 ml of complete media, using a 24-well plate format (BD Falcon), were incubated overnight to promote cell attachment and recuperation of the cell manipulation. Subsequently, cells were added with 100 µg/ml of rhLf and incubated for 24 h. In this series of experiments, the included controls were 5% v/v H_2O solvent control, untreated cells and as a positive control of apoptosis, cells treated with 2 mM of H_2O_2. Once that cells were collected and washed with ice-cooled PBS in a flow cytometric tube, they were dual stained by resuspending them with 100 µl of binding buffer containing annexin V-FITC and PI following manufacturer's recommendations (Beckman Coulter, Miami, FL). Briefly, after gentle homogenization, the cells resuspended with the staining mixture solution were incubated on ice for 15 min in the dark, and then, added with 300 µl of the ice-cold binding buffer, and immediately analyzed via flow cytometer (Gallios, Beckman Coulter) [33]. Approximately, 10,000 events (cells) were acquired for each sample. Two-parameter flow cytometric dot plots separated into four quadrants were utilized to acquire the percentages of apoptosis and necrosis values. For this purpose, the FL1 and FL2 detectors were placed along the *x*-axis and *y*-axis, respectively. For the interpretation of the four subpopulations provided by this type of analysis consult the following publications [26, 34]. All experimental points and controls were performed in quadruplicate. Data acquisition and analysis were accomplished by using Kaluza software (Beckman Coulter).

Examination rhLf effect on cell cycle profile via cellular DNA content and flow cytometry

The MDA-MB-231 cells seeded at a density of 25,000 cells/well in 1 ml of complete media were exposed to 6.76 and 9.48 µg/ml of rhLf for 72 h; 24-well plates were used for this purpose. Then, floating and adherent cells (detached with trypsin) were collected, centrifuged and gently resuspended in 100 µl of PBS. Then, added with 200 µl of nuclear isolation medium (NIM)-4,6-diamidino-2-phenylindole (DAPI) solution (NIM-DAPI; Beckman Coulter) and immediately processed via flow cytometry [26, 35]. Approximately, 20,000 events were acquired per sample by using a flow cytometer equipped with a 405 nm laser (Gallios; Beckman Coulter), a single cell gate and an FL9 detector. The analysis of cell cycle phase distribution was accomplished via Kaluza software (Beckman Coulter) by setting four gates in each single parameter histograms: as an indicator of apoptosis-induced DNA fragmentation, sub-G0/G1, hypodiploid; G0/G1, diploid; S, hyperdiploid; and G2/M, tetraploid [34]. Four replicas were performed for each experimental point and their associated controls.

Selective cytotoxicity index analysis

The selective cytotoxicity index (SCI) for rhLf was calculated as follow: SCI = CC_{50} of non-cancerous cells divided by CC_{50} of cancer cells. SCI denotes the capability of an experimental compound to kill cancer cells efficiently with minimal toxicity to non-cancerous cells [26]. SCI values

of 1 or less are suggestive of lack of selective cytotoxicity, whereas SCI values bigger than 1 are indicative of advantageous selective toxicity of the experimental compound towards cancer cells, as compared with non-cancerous cells [26]. SCI values > 1 are highly desired for any potential anticancer compound.

Statistical analysis

Two-tailed paired Student's *t* test was used to determine the statistical significances of two experimental samples (http://studentsttest.com/). A value of $P < 0.05$ was deemed significant to denote whether comparisons of two treatments have statistical significance. The results are depicted as an average with their corresponding standard deviation.

Results

Plasmid construct and rhLf purification

After *P. pastoris* transformation with pIGF5 carrying the hLf gene (Fig. 1), a selected colony was grown in a culture broth (see "Materials and methods"), the supernatant was collected, dialyzed and purified by using high-affinity Ni-charged resin affinity column. An aliquot of purified rhLf was analyzed by running an SDS-PAGE. After staining with Coomassie blue, the presence of a band of around 80 kDa was confirmed, which correspond to the molecular weight of human lactoferrin (Fig. 2a). Additionally, the presence of a single homogenous band equivalent to the molecular weight of hLf (~ 80 kDa) was confirmed with anti-his tag antibody and western blot analysis (Fig. 2b). These results indicate that the expression and purification of free-endotoxin rhLf from *P. pastoris* were accomplished, and suitable to perform further biological experiments.

Determination of the rhLf cytotoxic concentration 50% in human breast-derived cell lines

The cytotoxicity provoked by a concentration gradient of purified rhLf protein on MDA-MB-231, MDA-MB-231 LM2-4, and MCF-10A cell lines was quantified after 24 h of incubation. In Fig. 3 cytotoxicity percentages and representative images of live and dead cells used to quantify this percentage of experimental compound-mediated cytotoxicity in MDA-MB-231 cells are depicted. In this series of experiments, only cells derived from female donors were included, to circumvent the gender-related dissimilarities [27, 36, 37]. For this purpose, a live-cell DNS assay, validated for high throughput screening initiatives [28], and an IN Cell bioimager system (GE Healthcare) was used. To eliminate the cell death background, inherent to the cell culture manipulations, data were normalized by subtracting from each experimental

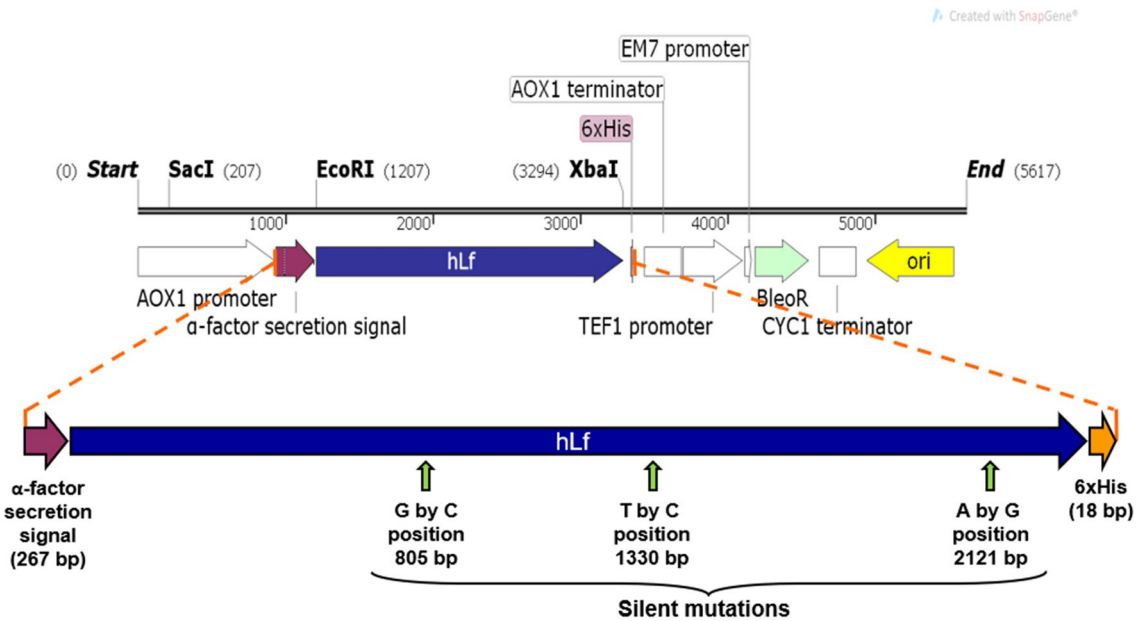

Fig. 1 The hLf open reading frame (ORF; 2136 bp) was cloned into pPICZα vector (Invitrogen), flanked by α-factor secretion signal and 6xHis tag, at 5′ and 3′ terminus, respectively. Additionally, several silent point mutations were introduced to eliminate undesired restriction sites and they are indicated by vertical arrows, including the nucleotide change and position (bp) in the rhLf ORF sequence. The resulting plasmid was named as pIGF5 (IGF-Iglesias Figueroa). AOX1, the alcohol oxidase 1 promoter from *P. pastoris*. The BleoR gene conferred the resistance to zeocin, a selective antibiotic for transformation

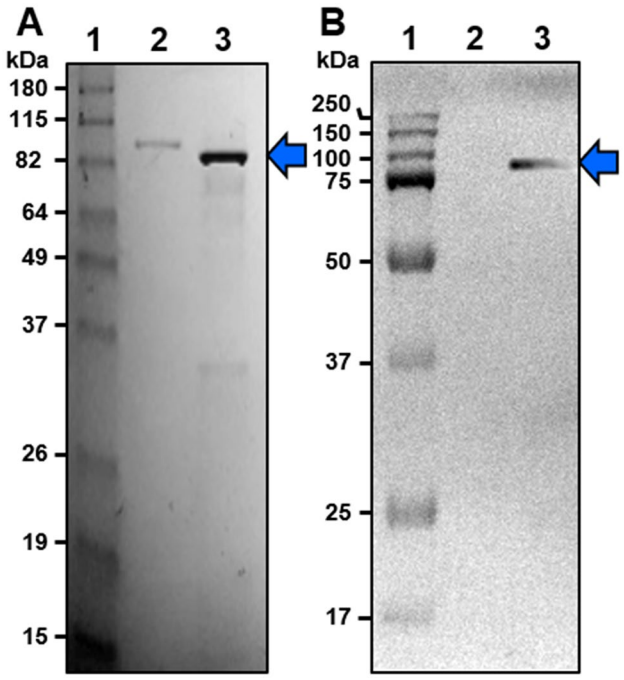

Fig. 2 The rhLf protein expression and purification analysis revealed the presence of a ~80 kDa protein via both SDA-PAGE (**a**) and western blots (**b**). Histidine (6x) tagged rhLf protein expressed in *P. pastoris* clone was purified from the yeast culture supernatant, by immobilized nickel affinity chromatography. After electrophoresis, an acrylamide gel was stained with Coomassie brilliant blue (**a**) and after western blotted was exposed to anti-his tag antibody (**b**): 1—molecular weight markers (MW) in kDa; 2—commercial bovine lactoferrin; 3—Histidine (6x) tagged rhLf protein partially purified; 4—a culture supernatant protein extracts from non-transformant *P. pastoris*, used as negative control

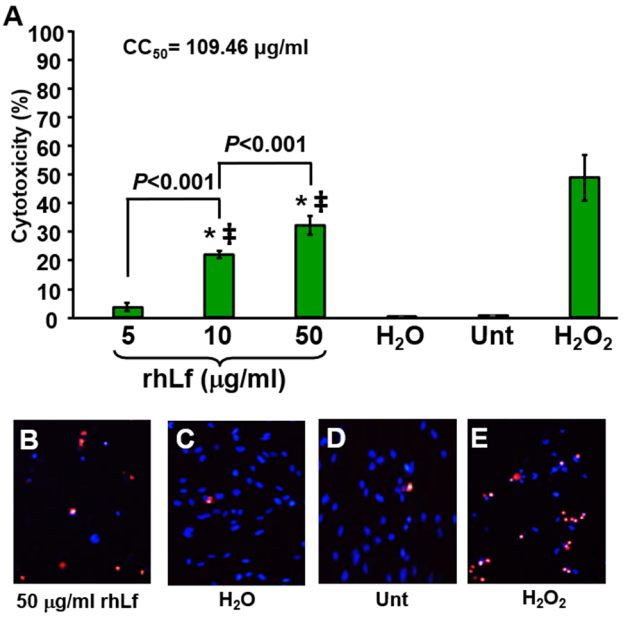

Fig. 3 The rhLf induces cytotoxicity on MDA-MB-231 cells in a dose-depended manner. Cells were exposed to a concentration gradient of rhLf and incubated for 24 h. Differential nuclear staining assay and a bioimager system were used to determine the cytotoxicity percentages (**a**; *y*-axis). When experimental samples were compared with solvent, 5% v/v H_2O, (*) and untreated control cells (‡), the *P* values were of <0.0001 and <0.0001, respectively (**a**). Cells treated with 2 mM of H_2O_2 were used as positive control for cytotoxicity (**a, e**). Each experimental point represents the average of four replicas and error bars their corresponding standard deviation (**a**). A portion of representative live-cell images, merging the Hoechst and propidium iodide (PI) channels, used to obtain the cytotoxic activity are depicted in **b**–**e**. Nuclei exhibiting a blue signal are considered to be living cells, whereas nuclei exhibiting magenta color, as a consequence of Hoechst and PI colocalization signal, are consider dead cells (**b**–**e**). Cytotoxic concentration 50% (CC_{50}; in µg/ml) is defined as the lactoferrin's concentration required to disrupt the plasma membrane of 50% of the cell population after 24 h of incubation. CC_{50} was calculated via linear interpolation (https://www.johndcook.com/interpolator.html)

value the percentage of cell death obtained from solvent control (H_2O)-treated cells, followed by calculating the CC_{50} by linear interpolation (https://www.johndcook.com/interpolator.html). Findings indicate that the rhLf CC_{50} values from MDA-MB231 and MDA-MB-231 LM2-4 cell lines were the lowest, being of 109.46 and 91.4 µg/ml and, respectively (Table 1). Also, the two additional triple negative cells, MDA-MB-468 and HCC70, displayed rhLf CC_{50} values of 491.8 and 823.6 µg/ml, respectively (Table 1). Furthermore, the rhLf CC_{50} values from MCF-7 cells was of 382.2 µg/ml, whereas the CC_{50} from T-47D cells was of 491.5 µg/ml (Table 1). Also, the rhLf CC_{50} obtained from non-cancerous epithelial MCF-10A cells was of 1279.48 µg/ml, being the highest as compared with all the breast cancer cells analyzed in this study (Table 1). Additionally, rhLf exhibited a favorable selective cytotoxicity index (SCI) on all six breast cancer cells tested, being the most effective of 11.68 and 13.99 for non-metastatic MDA-MB-231 and metastatic MDA-MB-231-LM2-4 cells, respectively (Table 1). Thus, the rhLf revealed to be similarly effective on non-metastatic MDA-MB-231 and metastatic MDA-MB-231-LM2-4 cells, with high favorable SCI values (more than 11), as compared with non-cancerous breast-derived MCF-10A cells (Table 1). Based on the above findings and due that is a prototype for the study of poorly differentiated hormone-independent breast cancer, the MDA-MB-231 cell line was selected for the next series of experiments.

Analyses of cellular morphological changes caused by rhLf on MDA-MB-231 cancer cells

The MDA-MB-231 triple negative breast cancer cells growing in 96-well plates were treated with 50 µg/ml of rhLf for 24 h, followed by Hoechst and PI DNS assay. In order to monitor cellular morphological changes, images were captured in a live-cell mode via a confocal microscope.

The results indicate that rhLf inflicts cell death, provoking morphological changes associated with apoptosis in MDA-MB-231 cells, such as cell shrinkage, blebbing and nuclear condensation (Fig. 4a–d). Interestingly, a fluorescent signal (reddish) inside of the blebs was visualized, most likely due to the presence of small DNA fragments that were released from the nuclei to the cytoplasm and forming complexes with PI (Fig. 4c, d). This observation suggests that rhLf is also able to cause apoptosis-induced DNA fragmentation. For comparison purposes, live-cell images from untreated/healthy MDA-MB-231 cells are depicted in Fig. 4e–h. Thus, based on cellular morphological changes, it appears that rhLf is using the apoptosis pathway, as a mechanism to inflict its cytotoxicity.

rhLf provokes an alteration of the cytoskeleton structure

Based on the above findings, the potential perturbing effect of rhLf on two major polymerized proteins forming the cytoskeletal structure, actin-microfilaments, and tubulin-microtubules, were analyzed via immunocytochemistry and confocal microscopy. For this purpose, the MDA-MB-231 and Hs27 cell lines were used. The inclusion of the human fibroblastic Hs27 cells as a control was due to their morphology, which is larger and flatter than breast-derived cells and their processes are elongated. Therefore, changes in their cytoskeleton structure are easier to be visually detected. Cells in 96-well plates were exposed to rhLf, followed by formaldehyde-fixation, Tween 20-permeabilization, and BSA-blocking procedures. Next, in a single step, cells were stained with anti-tubulin-Alexa 488 (green; microtubules), phalloidin-Alexa 568 (red; microfilaments) and DAPI (blue; nuclei). Subsequently, images were captured in three separate channels accordingly to the fluorophore's specifications. After 2 h of rhLf-treated MDA-MB-231 cells, it was noticed that the actin filamentous shape had disappeared. However, the Alexa-568 signal was detected to form an abundant punctuated pattern finely distributed in the whole cytoplasm of the cells (white arrows are just signaling three of these actin aggregations; Fig. 5a; Alexa-568 channel). In addition, cell size was appeared similar to the control cells after 2 h of exposure (Fig. 5d, e, h). On the other hand, the microtubules structure of the MDA-MB-231 cells appeared to be unaffected by rhLf (Fig. 5a). Nevertheless, after 4 h of rhLf exposure, the actin filamentous disorganization was more accentuated, forming larger and brighter amorphous F-actin clusters (red), considered as aggresomes [38, 39], localized toward the periphery of the cells, as compared with cells treated for 2 h of rhLf, as well as to the control cells (Fig. 5a, b, d, e, g). Concomitantly, cytosol shrinkage was evident at 4 h of incubation (4 h; Fig. 5b; Alexa-568 channel). To this point, the F-actin microfilament disruption provoked by rhLf on MDA-MB-231 cells resembles the alteration

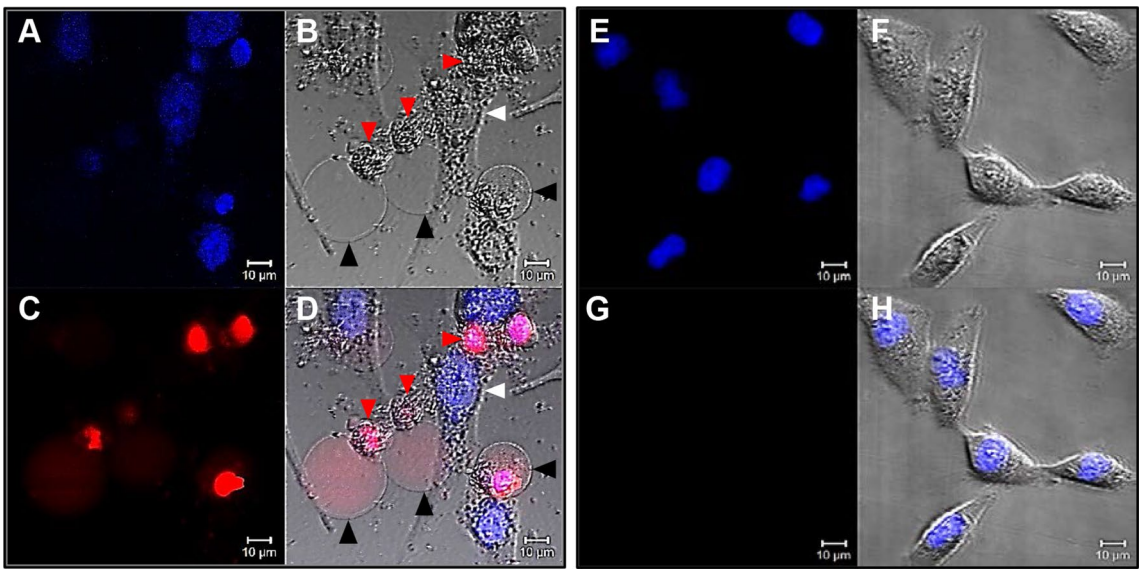

Fig. 4 The rhLf inflicts cell death, DNA fragmentation and morphological changes associated with apoptosis in MDA-MB-231 triple negative breast cancer cells. Cells were exposed to 50 µg/ml of rhLf for 24 h and double stained with Hoechst and PI. Representative live-cell confocal microscope images, captured using Hoechst channel (nuclei; **a**), brightfield differential interference contrast (DIC; **b**), propidium iodide channel (**c**) and overlay of the preceding three images (**d**), are depicted. The black head arrows are indicating the blebs formation, whereas the redhead arrows are denoting cell shrinkage and chromatin condensation, dead cells, PI positive. Also, the white head arrow is signaling a cell with a non-condensed nucleus, non-cell shrinkage and non-blebs formation, as well as PI negative, therefore a living cell. Also, as above, live-cell images from untreated cells are depicted as follow: **e** Hoechst channel (nuclei); **f** brightfield; **g** propidium iodide channel; and overlay of the preceding three images (**h**). Scale bar = 10 µm

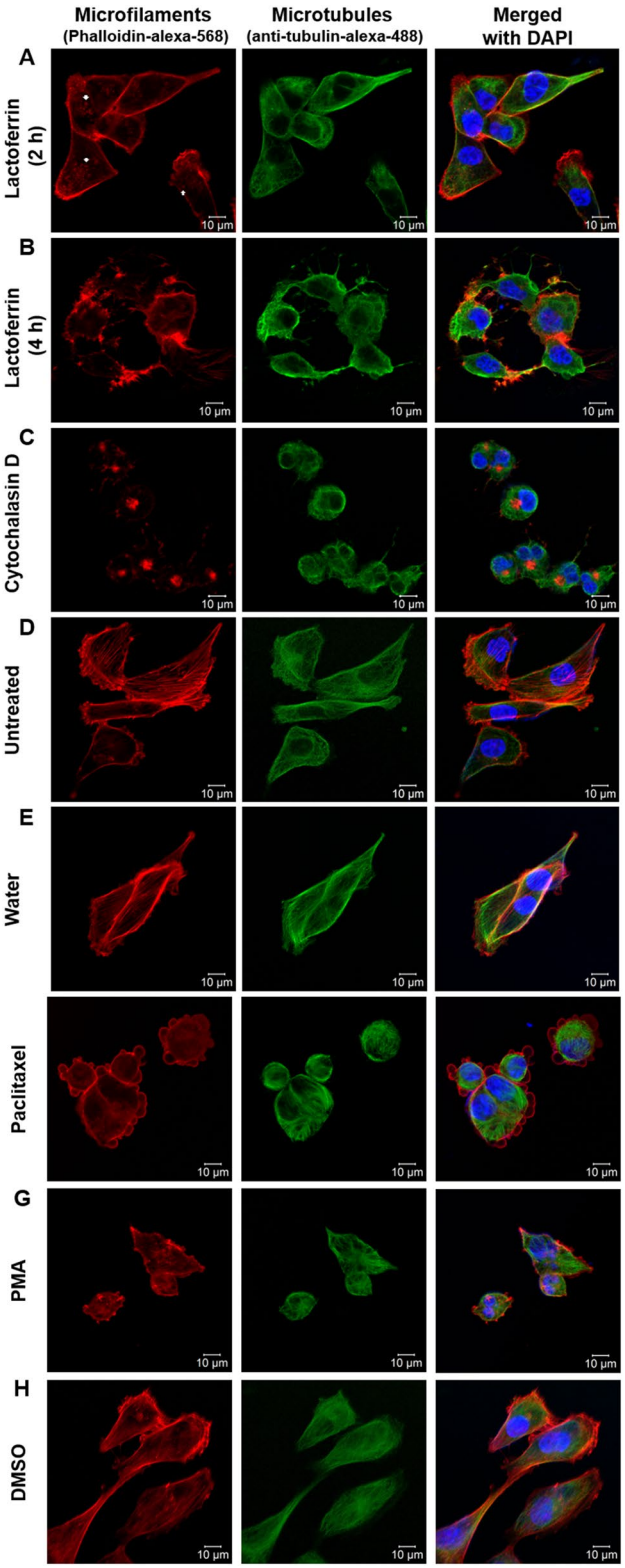

Fig. 5 The rhLf disrupted the F-actin (filamentous) cytoskeleton organization of MDA-MB-231 cells. Representative immunofluorescence confocal microscopy images of MDA-MB-231 cells, triple stained with Alexa-568-conjugated phalloidin, Alexa-488 anti-tubulin, and DAPI, displaying the microfilaments (actin; Alexa-568 channel) and microtubules (tubulin; Alexa-488 channel) organization and nucleus (blue channel), respectively. Cells were treated as follow: **a** for 2 h with rhLf; **b** for 4 h with rhLf; **c** with cytochalasin D; **d** untreated; **e** with H_2O solvent control; **f** with paclitaxel; **g** with DMSO solvent control. The left column of images correspond to the F-actin microfilaments (red), and the center column microtubules (green) and the right column merged images of the Alexa-568 and Alexa-488 channels with DAPI (blue; nuclei) channel

profile induced by cytochalasin D (Fig. 5b, c; Alexa-568 channel), which also caused large cytoplasmic F-actin aggregation. However, these F-actin aggregates induced by cytochalasin D on MDA-MB-231 were mainly localized in the nuclear periphery space (Fig. 5c; Alexa-568 channel and merged image). When analyzing the effect of rhLf on Hs-27 fibroblasts, a similar pattern was seen to the one detected in MDA-MB-231 cells, with loss of actin microfilaments organization and abundant punctuated F-actin clusters in the cytoplasm (white arrows; Fig. 6a; Alexa-568 channel). In rhLf-treated Hs-27 cells, also as was seen in MDA-MB-231 the microtubules organization was visually unchanged (Fig. 6a; Alexa-488 channel). As expected, cytochalasin D-treated Hs-27 cells exhibited a distorted microfilament organization, provoking cytoplasmic F-actin aggresomes formation (white arrows; Fig. 6b; Alexa-488 channel). As expected, both paclitaxel-treated MDA-MB-231 and Hs-27 cells showed microtubule shortening without disrupting their filamentous shape (Figs. 5f, 6e; Alexa-488 channels) or decreasing the cell size. In addition, paclitaxel caused blebbing on MDA-MB-231 cells (Fig. 5f; white arrows). Consistently, DMSO-treated, H_2O-treated and untreated control cells displayed unaltered organization in both microfilaments and F-actin microtubules structure (Figs. 5d, e, h, 6c, d, f; respectively). Thus, these analyses revealed that rhLf provoked disorganization of the cytoskeleton architecture by altering the F-actin microfilaments network, as evidenced by the disappearance of filamentous actin (F-actin), concomitant with aggresomes formation, in both MDA-MB-231 and Hs27 cells. Moreover, the increased changes in punctuated F-actin filaments aggregation exerted by rhLf occurred in a time-depended manner on MDA-MB-231 cells.

rhLf elicits phosphatidylserine externalization on breast cancer-derived MDA-MB-231 cells

The rhLf mechanism of action was examined in more detail by analyzing an early biochemical event in cells undergoing apoptosis, the externalization of phosphatidylserine (PS) to the outer leaflet of the plasma membrane; an early hallmark of apoptosis [40]. MDA-MB-231 cells were treated with rhLf (100 µg/ml) for 24 h, followed by staining with annexin V-FITC and PI and their fluorescence signal was then monitored via flow cytometry [29]. As expected, rhLf preferentially induced apoptosis (28.3%), as compared to necrosis

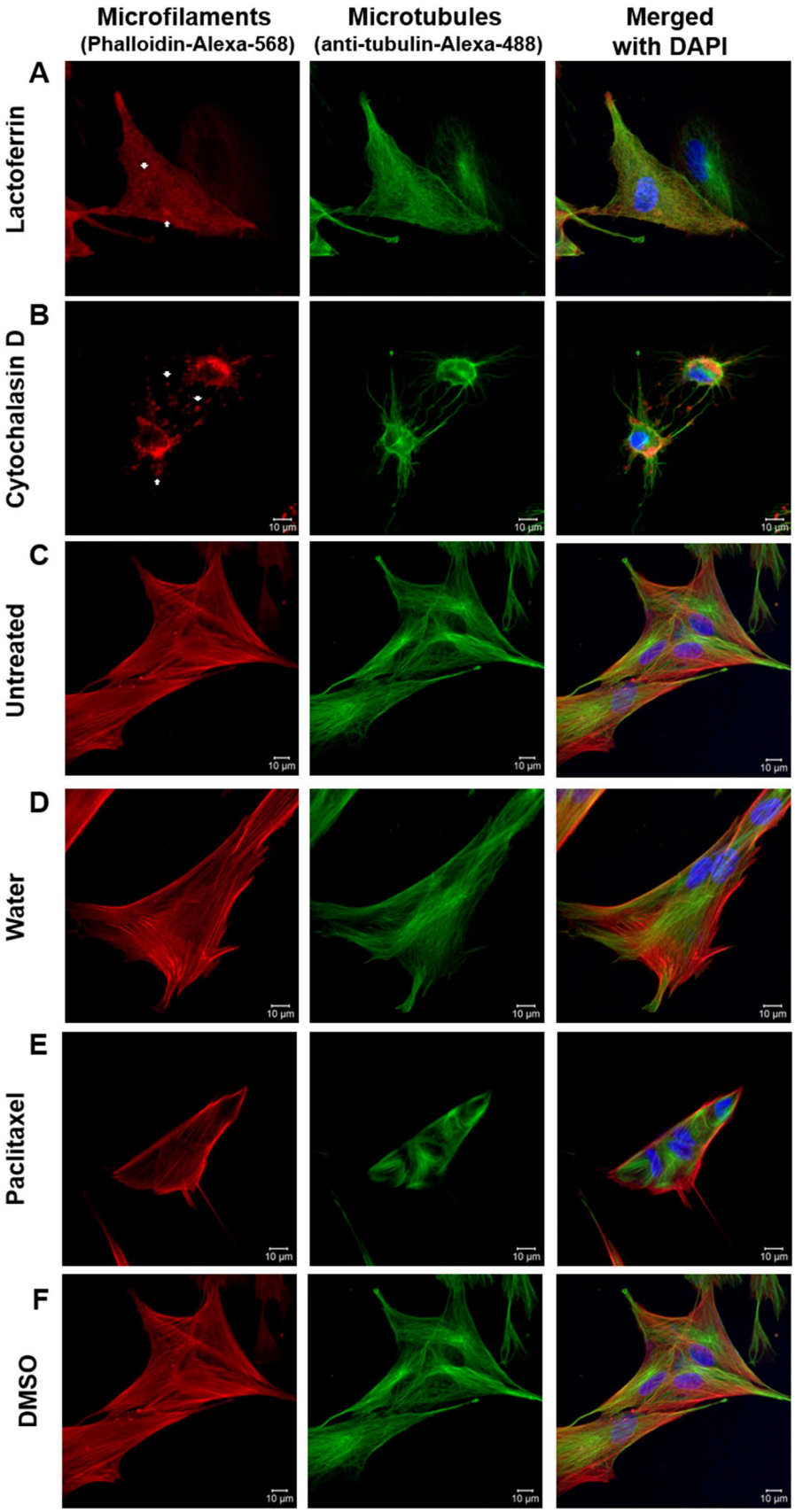

Fig. 6 The rhLf disturbed the F-actin (filamentous) cytoskeleton organization of Hs27 cells. Representative immunofluorescence confocal microscopy images of Hs27 cells, triple stained with Alexa-568-conjugated phalloidin, Alexa-488 anti-tubulin, and DAPI, displaying the microfilaments (actin; Alexa-568 channel) and microtubules (tubulin; Alexa-488 channel) organization and nucleus (blue channel). Cells were treated as follow: **a** with rhLf; **b** with cytochalasin D; **c** untreated; **d** with H_2O solvent control; **e** with paclitaxel; **f** with DMSO solvent control. The left column of images correspond to the F-actin microfilaments (red), the center column microtubules (Alexa-488) and the right column merged images of the Alexa-568 and Alexa-488 channels with DAPI (blue; nuclei) channel

(0.85%) in MDA-MB-231 cells (Fig. 7). Furthermore, after the apoptotic percentages of rhLf-treated cells were compared with H_2O-treated and untreated cells, the *P* values were of 0.004123 and 0.002712, respectively (Fig. 7). Cells treated with solvent control (H_2O) and the untreated cells did not display a substantial increase in both apoptosis and necrosis percentages (Fig. 7). As expected, the H_2O_2-treated cells (2 mM) showed a high percentage of apoptosis cells (53.62%). Thus, these findings suggest that rhLf is utilizing the apoptotic pathway to inflict its cytotoxicity, as evidenced by the PS externalization.

rhLf induces DNA fragmentation and alters the cell cycle of MDA-MB-231 cells

To gain insight into the potential mechanisms used by rhLf to inhibit cell proliferation and/or to induce cytotoxicity, analyses of the cell cycle profile were performed. For this initiative, MDA-MB-231 cells were treated with the rhLf CC_{10} (6.76 µg/ml) and CC_{20} (9.48 µg/ml) for 72 h, followed by their permeabilization and staining for analysis via flow cytometry [26, 35, 41]. Here, the cell cycle analysis was centered on differences in the cellular DNA content based on a nuclear isolation medium (NIM)-4,6-diamidino-2-phenylindole (DAPI) solution (NIM-DAPI; Beckman Coulter) and recording their fluorescence signal intensity via a Gallios flow cytometer [26, 35, 41]. The amount of DAPI emission fluorescence signal is directly proportional to the cellular

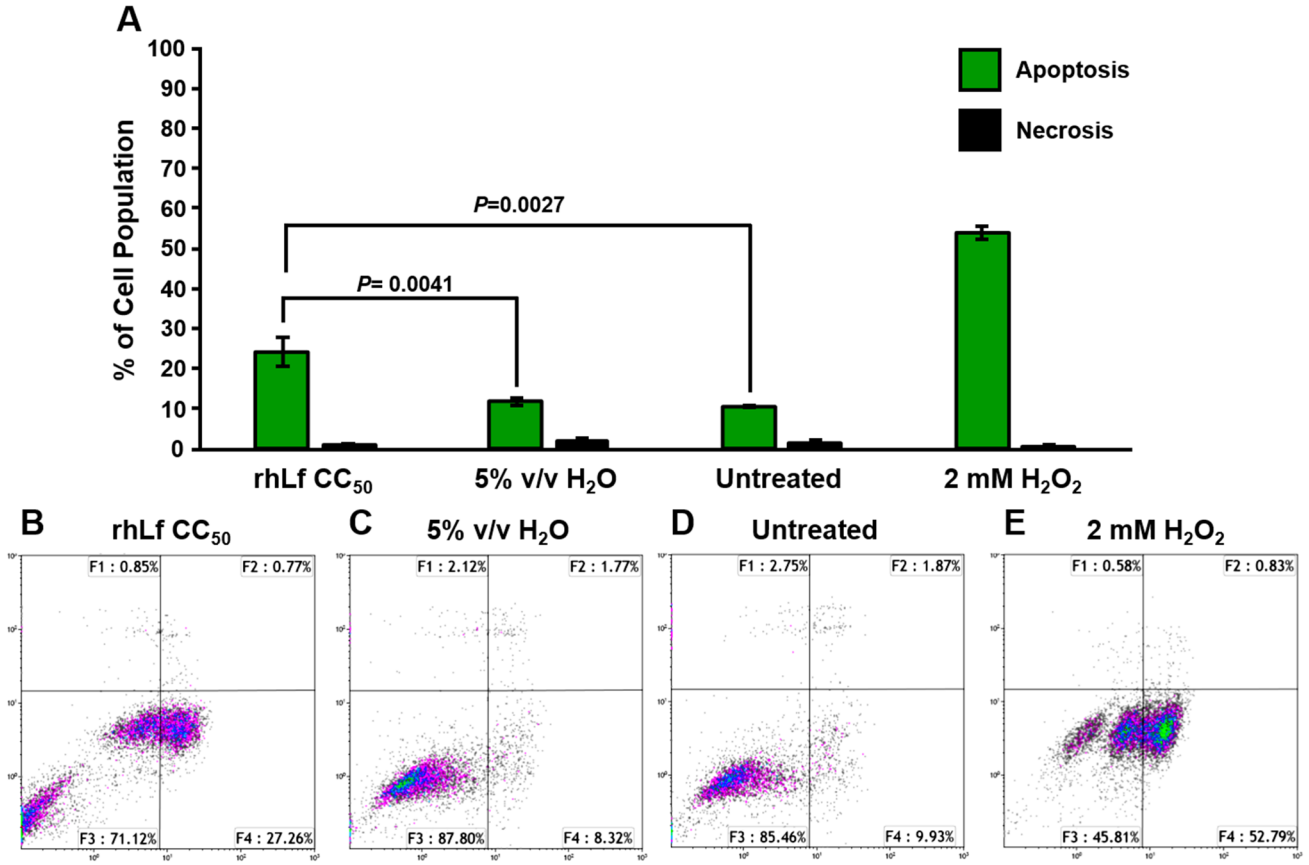

Fig. 7 The rhLf evokes significant phosphatidylserine externalization on MDA-MB-231 cells after 24 h of incubation. The rhLf mechanism of inflicting cell death, apoptosis or necrosis, was examined after cells were double stained with annexin V-FITC and PI and monitored via flow cytometry. The total percentage of apoptotic cell populations (*y*-axis) is expressed as the sum of both early and late stages of apoptosis (green bars), whereas that cells stained only with PI, were considered as necrotic cell population (also in y-axis; black bars; **a**). Each bar represents the average of four independent measurements, and error bars their corresponding standard deviation (**a**). Representative two-parameter flow cytometry dot plots used to acquire the percentages of apoptotic and necrotic subpopulations (**b**–**e**). The following controls were included: cells treated with 5% v/v of H_2O, as a solvent control (**a, c**); untreated cells as negative controls (**a, d**); and cells exposed to 2 mM of H_2O_2, as a positive control for cytotoxicity (**a, e**); analysis using two-tailed Student's paired *t* test are included as *P* values (**a**). Approximately, 10,000 events (cells) were acquired per sample. For acquisition and analysis purposes, Kaluza flow cytometry software was used (Beckman Coulter)

DNA content. Results indicated that the percentage of the sub-G0/G1 subpopulation from cells treated with 6.76 µg/ml of rhLf was similar to the solvent (H_2O) and untreated control cells (Fig. 8a, e, f, h). In contrast, cells exposed to 9.48 µg/ml of rhLf displayed a higher percentage of the sub-G0/G1 subpopulation (6%) and was deemed significant as compared with solvent and untreated control cells, with *P* values of 0.00033 and 0.00016, respectively (Fig. 8a, e, f, h). This sub-G0/G1 subpopulation (hypodiploid) is an indicator of apoptosis-induced DNA fragmentation [34, 41]. In addition, these results support the assumption made during the morphological changes analysis via confocal microscopy experiments (above), indicating that the fluorescent signal inside of the blebs was probably due to the presence of small

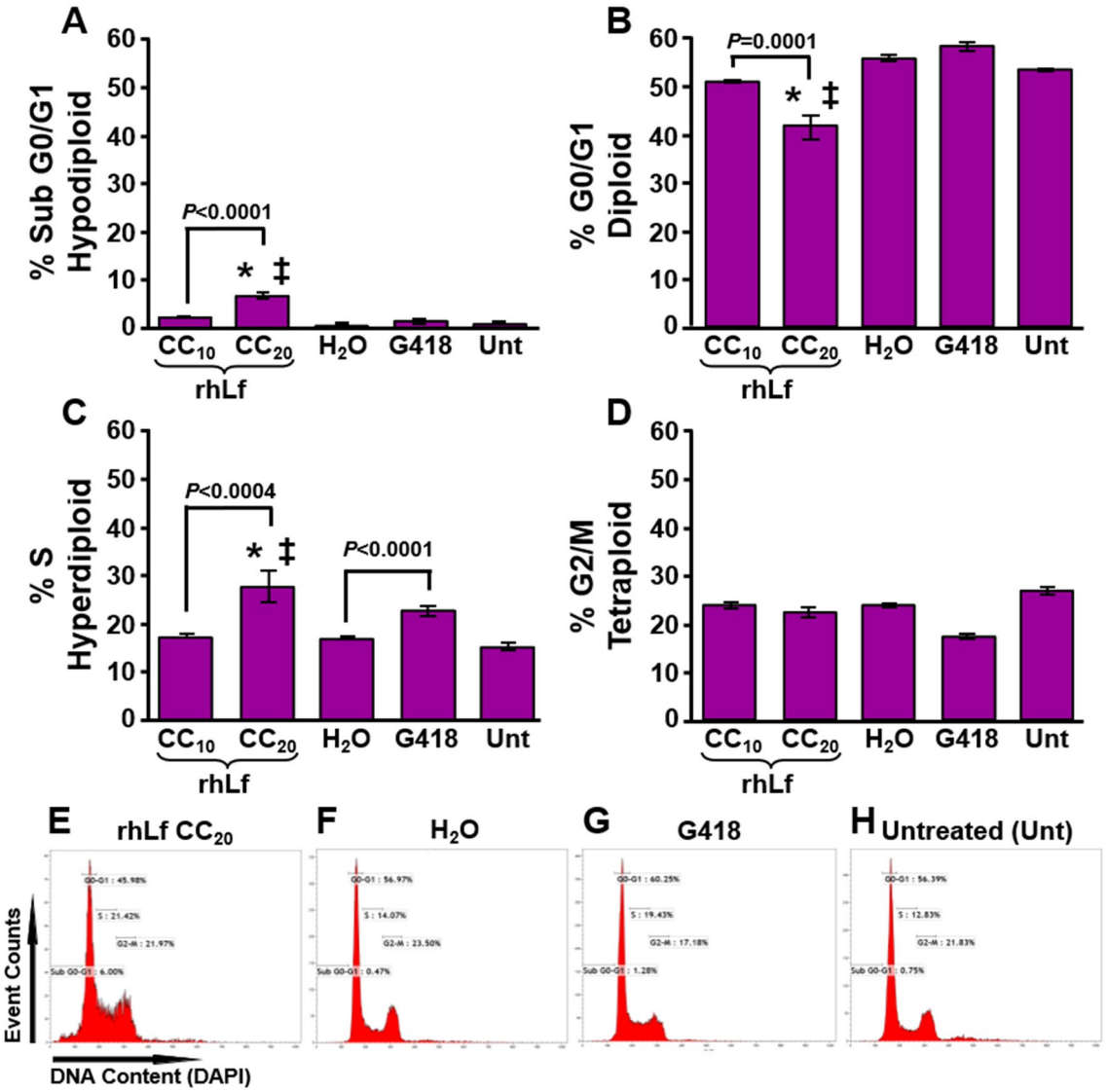

Fig. 8 The rhLf provoked apoptosis-induced DNA fragmentation and alteration of the cell-cycle distribution profile on MDA-MB-231 cells after 72 h of incubation. Cells were collected, and in a single step were fixed, permeabilized, and DAPI-stained, followed by an examination via flow cytometer. **a**–**d** The quantification of event/cell frequency percentages is included along with the y-axis, whereas the different treatments are plotted along the horizontal *x*-axis. Controls for this series of experiments included: as a solvent control, 5% v/v H_2O; as a positive control of cell cycle perturbation, 1 mg/ml of G418; and untreated cells. Each bar represents an average of four replicates, and the error bars signify their corresponding standard deviation. The significance difference (Student *t* test) between rhLf CC_{20} (9.48 µg/ml) vs. H_2O-treated (*) or untreated (‡) cells were consistent with $P < 0.01$, respectively. **e**–**h** Representative single-parameter histograms, including four gates that encompassed the percentage of each cell subpopulation per phase of the cell cycle. Gates from left to right: sub-G0/G1, counted as apoptotic DNA fragmentation; G0/G1, S, and G2/M. **e**–**h** Event (cells) counts are plotted along the y-axis, whereas DNA content is along the x-axis. Kaluza flow cytometry software was used for sample acquisition and analysis purposes (Beckman Coulter)

DNA fragments-PI complexes. The percentages at G0/G1 phase (diploid; 2N) obtained from 9.48 µg/ml rhLf-treated cells (45.98%) was significantly reduced ($P < 0.01$), as compared with H_2O-treated (56.97%) and untreated (56.39%) cells (Fig. 8b, e, f, h). Significant differences in the S phase (hyperdiploid) subpopulations of 9.48 µg/ml rhLf-treated cells were found, when compared with cells exposed to 6.76 µg/ml of rhLf ($P = < 0.0004$), as well as to solvent and untreated controls, respectively ($P < 0.01$; Fig. 8c, e, f, h). Notably, this increment in the S phase subpopulation pattern provoked by rhLf resembled the arrest profile induced by the inhibitor of polypeptide synthesis, G418 (Fig. 8c, e, g). Cells exposed to rhLf with a G2/M DNA content (tetraploid; 4N), displayed similar percentage values as the solvent and untreated controls, and therefore, non-significant differences were obtained (Fig. 8d, f, h). Based on this analysis strategy, results suggest that rhLf is able to provoke apoptosis-induced DNA fragmentation, and also, to arrest the cells in the S phase, altering the normal cell cycle progression. Moreover, both events occurred in a pronounced dose-dependent modality.

Discussion

Breast cancer is the most frequent malignancy diagnosed in women worldwide. Therefore, in this study, rhLf was tested for its capability to kill a panel of six human breast cancer cell lines in vitro. Additionally, the mechanism used by rhLf was partially investigated. Moreover, by including a human non-cancerous epithelial cell line from breast and female origin, it was possible to investigate whether rhLf possess selective cytotoxicity (SCI) against breast cancer cells. Results revealed that rhLf kills efficiently both non-metastatic and metastatic cells with similar CC_{50} values (109.46 and 91.4 µg/ml, respectively), with much less noticeable toxicity on non-cancerous MCF-10A cells (CC_{50} of 1279.48 µg/ml); a more than 11-folds difference (SCI). In addition, rhLf also exerted cytotoxicity on four additional human breast cancer cell lines, MDA-MB-468, HCC70, MCF-7 and T-47D, with CC_{50} values (382.2–823.6 µg/ml) higher than those displayed on MDA-MB-231 cells. Thus, the six breast cancer cell lines examined in this study exhibiting dissimilar hormonal receptors, including three triple-negative cell lines (MDA-MB-231, MDA-MB-468 and HCC70), were differently affected after rhLf exposure. These findings suggest that the cytotoxic profile exerted by rhLf on breast cancer cells could be hormone-independent breast cancer receptors.

A crucial reason why cancer cells are highly challenging to treat is due to their high rate of proliferation. Finding novel experimental compounds that specifically kill cancer cells, with little, if any, activity on normal cells is highly desirable. Therefore, it is important to compare the cytotoxicity of a new experimental drug or compound on cancer and non-cancerous ("normal") cell lines, to acquire its selective cytotoxicity by calculating its SCI. When the SCI value of an experimental compound is higher than 1, the compound is considered possessing selective cytotoxic against cancer cells [26]. A favorable SCI means that the experimental compound is effective in killing cancer cells while causing a minimal or no toxicity on normal (non-cancerous) cells, a preferred characteristic to validate the effectiveness of a potential anticancer drug [26, 41]. In a previous work by Yang et al. [10], indicated that bovine lactoferrin (bLf) possessed selective cytotoxicity on breast cancer cells, as compared with MCF-10A cells, however, the SCI value was not included. In addition, Pereira et al. [42], claimed that bLf has selective cytotoxicity via apoptosis on breast cancer cells, however, the SCI value was also not determined. In this study, rhLf exhibited selective cytotoxicity on non-metastatic and metastatic MDA-MB-231 cells (11.68 and 13.99, respectively). Also, the SCI values displayed by rhLf on four additional human breast cancer cell lines, MDA-MB-468, HCC70, MCF-7 and T-47D, were suitable (1.55–3.34). Therefore, rhLf is an attractive anti-breast cancer drug.

Apoptosis is a multifaceted process implicating several morphological changes, like plasma membrane blebbing, cell shrinkage, and nuclear condensation. Using fluorescence staining (Hoechst and PI; DNS assay) and confocal microscopy the potential morphological changes induced by rhLf on MDA-MB-231 cells were visualized. A previous study has shown that bLf was unable to provoke morphological changes associated with apoptosis in MDA-MB-231 cells [43]. Conversely, in this study, findings indicated that rhLf was able to induce morphological changes associated with apoptosis in MDA-MB-231 cells, like cell shrinkage, plasma membrane blebbing and nuclear condensation (Fig. 4). Additionally, during this analysis, a fluorescence signal was observed inside of the blebs, probably due to the presence of DNA fragments forming complexes with PI and Hoechst, since both are DNA intercalators dyes.

These observations encouraged us to investigate the potential participation of the cytoskeleton in these cellular morphological changes. A plasma membrane bleb is the development of bubble-like cell-surface protrusion occurring by losing contact between the cytoskeleton proteins and the plasma membrane during apoptosis [44]. To validate whether the cytotoxicity provoked by rhLf involved the cytoskeleton disorganization on MDA-MB-231 and Hs27 cells, fluorescence confocal microscopy analyses were conducted. The rhLf-exposed cells were labeled to detect the two major polymerized proteins forming the cytoskeleton, F-actin and tubulin, microfilaments and microtubules, respectively. These assays revealed that rhLf caused uncoupling of the normal cytoskeleton organization by disturbing

the F-actin microfilaments network, concomitant with formation of an irregular cytoplasmic punctuated pattern (aggresomes), in both MDA-MB-231 and Hs27 cells. Interestingly, a similar F-actin perturbation effect was induced by bLf on breast T-47D cells [42].

Under homeostasis, the distribution of phospholipids is asymmetric in the plasma membrane of eukaryotic cells. This asymmetrical distribution of phospholipids has important functions in vivo [45]. Normally phosphatidylserine (PS) is predominantly confined to the cytoplasmic leaflet of the plasma membrane and disruption of this asymmetry, leading to externalization of PS to the surface of the cell, play a central role as a recognition signal to activate phagocytes and to promote the blood coagulation cascade; and is a well-established biochemical hallmark in apoptosis [46]. This event is easily detected by using an annexin V protein (~ 36 kDa), which possess a high affinity for PS. Moreover, when using the double annexin V-FITC and PI staining approach and flow cytometry, it is possible to discern whether a cytotoxic experimental compound is using the apoptosis or necrosis pathway to inflict its cell death. Previous studies have demonstrated that by using bLf and breast cancer cell lines, no apoptotic cells with PS externalized were detected after a 72 h period of treatment [43]. In another study, PS externalization induced by bLf in breast cancer Hs 578T and MDA-MB-231 cell lines after 48 h of treatment was detected [42]. More recently, it was reported that bLf activated apoptosis via PS externalization in prostate cancer PC-3 and osteosarcoma MG-63 cells after 48 h and 72 h of incubation, respectively [47]. In our study, rhLf elicited significant PS externalization ($P = 0.004$) on triple negative MDA-MB-231 cells after 24 h of exposure. This result suggests that rhLf expressed in *P. pastoris* is able to induce apoptosis.

We next sought to analyze the cell cycle profile to further elucidate in more detail the mechanism that rhLf uses to inflict its cytotoxic effect. A late biochemical event in cells experiencing apoptosis is their DNA fragmentation, which is mainly provoked by an endogenous caspase-3-activated deoxyribonuclease (CAD), during the execution phase of apoptosis [48]. In this biochemical event, CAD causes degradation of chromatin, generating small fragments of DNA that diffuse out of the nucleus, originating a cell subpopulation with hypodiploid DNA content easily detected via flow cytometry during cell cycle analysis. This sub-G0/G1 (hypodiploid) subpopulation appears to the left side of the single parameter (DAPI; FL-9 detector) flow cytometric histograms and it is interpreted as cells experiencing apoptosis-induced DNA fragmentation [34, 49]. A previous report indicated that bovine Lf caused cell cycle arrest in several breast cancer cell lines, however, this arrest was in the G2 phase for the MDA-MB-231 cells [43]. In that study, no fraction of cells at the sub-G0/G1 phase was detected. In addition, in head and neck cancer cells rhLf arrested the cell cycle at the G0/G1 checkpoint [50]. Moreover, rhLf caused growth arrest at the G1 to S transition on breast MDA-MB-231 cells [51]. Here, we confirmed that rhLf indeed causes the arrest of the cell cycle, at the S phase in MDA-MB-231 cells, resembling the pattern displayed by the G418 inhibitor of polypeptide synthesis included as a control in this series of experiments. Furthermore, in our hands rhLf was also able to elicit DNA fragmentation, as evidenced by an increase of the sub-G0/G1 subpopulation, supporting the above morphological observations where a fluorescence signal was detected inside of the plasma membrane blebs. Thus, our results suggest that rhLf alters the cell cycle and induces DNA fragmentation.

In conclusion, our findings demonstrate that rhLf expressed in *P. pastoris* elicited effective toxicity on a highly malignant and aggressive non-metastatic and metastatic human triple negative MDA-MB-231 cells, with favorable SCI values, as compared with human non-cancerous epithelial MCF-10A cells. In addition, our rhLf elicited morphological and biochemical characteristics of apoptosis on MDA-MB-231 cells. These morphological alterations included plasma membrane blebbing, probably linked to the disappearance of F-actin shape structures, cell shrinkage and nuclear/chromosome condensation, being all three apoptosis-associated morphological changes. In addition, the biochemical alterations provoked by rhLf in MDA-MB-231 cells included PS externalization, apoptosis-induced DNA fragmentation, and arrest of the cell cycle progression; all hallmarks of apoptosis. Our data suggest that rhLf could be useful in controlling effectively the proliferation of human breast cancer cells, with minimum damage to normal cells. Furthermore, the rhLf anti-breast cancer activity merits to be tested on an animal model.

Acknowledgements BFIF thank the Consejo Nacional de Ciencia y Tecnología (CONACyT) for the Ph.D. studies grant. Funding for this work was supported by an internal grant (2016-2017) from the Facultad de Ciencias Químicas, the Universidad Autónoma de Chihuahua to QRC, and also, partially provided by the National Institute of General Medical Sciences-Support of Competitive Research (SCORE) grant 1SC3GM103713 to RJA. The authors thank the Cytometry, Screening and Imaging, the Biomolecule Analysis and the Genomic Analysis Core Facilities at the University of Texas at El Paso (UTEP). Those Core Facilities were supported by a Research Centers in Minority Institutions (RCMI) program grant 5G12MD007592 to the Border Biomedical Research Center (BBRC) in UTEP from the National Institute on Minority Health and Health Disparities, a component of the National Institutes of Health. The authors also thank Gladys Almodovar and Lisett Contreras (both with UTEP) for outstanding technical and cell culture expertise and to Professor Giulio Francia (with UTEP) for the generous gift of the MDA-MB-231/LM2-4 cell line.

Compliance with ethical standards

Conflict of interest The authors declare no conflict of interest.

References

1. Actor JK, Hwang S-A, Kruzel ML (2009) Lactoferrin as a natural immune modulator, Curr Pharm Des 15:1956
2. Van der Strate B, Harmsen M, Schäfer P, Swart P, Jahn G, Speer C, Meijer D, Hamprecht K (2001) Viral load in breast milk correlates with transmission of human cytomegalovirus to preterm neonates, but lactoferrin concentrations do not. Clin Diagn Lab Immunol 8:818–821
3. Iglesias-Figueroa BF, Espinoza-Sánchez EA, Siqueiros-Cendón TS, Rascón-Cruz Q (2018) Lactoferrin as a nutraceutical protein from milk, an overview, Int Dairy J. https://doi.org/10.1016/j.idairyj.2018.09.004
4. García-Montoya IA, Cendón TS, Arévalo-Gallegos S, Rascón-Cruz Q (2012) Lactoferrin a multiple bioactive protein: an overview. Biochim Biophys Acta (BBA)-Gen Subj 1820:226–236
5. Siqueiros-Cendón T, Arévalo-Gallegos S, Iglesias-Figueroa BF, García-Montoya IA, Salazar-Martínez J, Rascón-Cruz Q (2014) Immunomodulatory effects of lactoferrin. Acta Pharmacol Sin 35:557–566
6. Giansanti F, Panella G, Leboffe L, Antonini G (2016) Lactoferrin from milk: nutraceutical and pharmacological properties. Pharmaceuticals 9:61
7. W.O. (2019) "WHO | Cancer. http://www.who.int/news-room/fact-sheets/detail/cancer. Accessed 19 Feb 2019
8. American Cancer Society, Cancer Facts & Figures (2019). https://www.cancer.org/research/cancer-facts-statistics/all-cancer-facts-figures/cancer-facts-figures-2019.html. Accessed 19 Feb 2019
9. Abu-Serie MM, El-Fakharany EM (2017) Efficiency of novel nanocombinations of bovine milk proteins (lactoperoxidase and lactoferrin) for combating different human cancer cell lines. Sci Rep 7:16769
10. Zhang Y, Lima CF, Rodrigues LR (2014) Anticancer effects of lactoferrin: underlying mechanisms and future trends in cancer therapy. Nutr Rev 72:763–773
11. Yang N, Rekdal Ø, Stensen W, Svendsen J (2002) Enhanced antitumor activity and selectivity of lactoferrin-derived peptides. J Pept Res 60:187–197
12. de Mejia EG, Dia VP (2010) The role of nutraceutical proteins and peptides in apoptosis, angiogenesis, and metastasis of cancer cells. Cancer Metastasis Rev 29:511–528
13. Rosa L, Cutone A, Lepanto MS, Paesano R, Valenti P (2017) Lactoferrin: a natural glycoprotein involved in iron and inflammatory homeostasis. Int J Mol Sci 18:1985
14. Kazan HH, Urfali-Mamatoglu C, Gunduz U (2017) Iron metabolism and drug resistance in cancer. Biometals 30:629–641
15. Legendre C, Garcion E (2015) Iron metabolism: a double-edged sword in the resistance of glioblastoma to therapies. Trends Endocrinol Metab 26:322–331
16. Dixon SJ, Lemberg KM, Lamprecht MR, Skouta R, Zaitsev EM, Gleason CE, Patel DN, Bauer AJ, Cantley AM, Yang WS (2012) Ferroptosis: an iron-dependent form of nonapoptotic cell death. Cell 149:1060–1072
17. Yang WS, SriRamaratnam R, Welsch ME, Shimada K, Skouta R, Viswanathan VS, Cheah JH, Clemons PA, Shamji AF, Clish CB (2014) Regulation of ferroptotic cancer cell death by GPX4. Cell 156:317–331
18. Iglesias-Figueroa B, Valdiviezo-Godina N, Siqueiros-Cendón T, Sinagawa-García S, Arévalo-Gallegos S, Rascón-Cruz Q (2016) High-level expression of recombinant bovine lactoferrin in *Pichia pastoris* with antimicrobial activity. Int J Mol Sci 17:902
19. Cailleau R, Young R, Olive M, Reeves W Jr (1974) Breast tumor cell lines from pleural effusions. J Natl Cancer Inst 53:661–674
20. Munoz R, Man S, Shaked Y, Lee CR, Wong J, Francia G, Kerbel RS (2006) Highly efficacious nontoxic preclinical treatment for advanced metastatic breast cancer using combination oral UFT-cyclophosphamide metronomic chemotherapy. Cancer Res. 66:3386–3391
21. Cailleau R, Olive M, Cruciger QV (1978) Long-term human breast carcinoma cell lines of metastatic origin: preliminary characterization. In vitro 14:911–915
22. Lee AV, Oesterreich S, Davidson NE (2015) MCF-7 cells—changing the course of breast cancer research and care for 45 years. JNCI: J Natl Cancer Inst. https://doi.org/10.1093/jnci/djv073
23. Gazdar AF, Kurvari V, Virmani A, Gollahon L, Sakaguchi M, Westerfield M, Kodagoda D, Stasny V, Cunningham HT, Wistuba II (1998) Characterization of paired tumor and non-tumor cell lines established from patients with breast cancer. Int J Cancer 78:766–774
24. Keydar I, Chen L, Karby S, Weiss F, Delarea J, Radu M, Chaitcik S, Brenner H (1979) Establishment and characterization of a cell line of human breast carcinoma origin. Eur J Cancer (1965) 15:659–670
25. Soule HD, Maloney TM, Wolman SR, Peterson WD, Brenz R, McGrath CM, Russo J, Pauley RJ, Jones RF, Brooks S (1990) Isolation and characterization of a spontaneously immortalized human breast epithelial cell line, MCF-10. Cancer Res 50:6075–6086
26. Robles-Escajeda E, Das U, Ortega NM, Parra K, Francia G, Dimmock JR, Varela-Ramirez A, Aguilera RJ (2016) A novel curcumin-like dienone induces apoptosis in triple-negative breast cancer cells. Cellular Oncol 39:265–277
27. Nunes LM, Robles-Escajeda E, Santiago-Vazquez Y, Ortega NM, Lema C, Muro A, Almodovar G, Das U, Das S, Dimmock JR (2014) The gender of cell lines matters when screening for novel anti-cancer drugs. AAPS J 16:872–874
28. Lema C, Varela-Ramirez A, Aguilera RJ (2011) Differential nuclear staining assay for high-throughput screening to identify cytotoxic compounds. Curr Cell Biochem 1:1
29. Varela-Ramirez A, Costanzo M, Carrasco YP, Pannell KH, Aguilera RJ (2011) Cytotoxic effects of two organotin compounds and their mode of inflicting cell death on four mammalian cancer cells. Cell Biol Toxicol 27:159–168
30. Santiago-Vázquez Y, Das U, Varela-Ramirez A, Baca ST, Ayala-Marin Y, Lema C, Das S, Baryyan A, Dimmock JR, Aguilera RJ (2016) Tumor-selective cytotoxicity of a novel pentadiene analogue on human leukemia/lymphoma cells. Clin Cancer Drugs 3:138–146
31. Gutierrez DA, DeJesus RE, Contreras L, Rodriguez-Palomares IA, Villanueva PJ, Balderrama KS, Monterroza L, Larragoity M, Varela-Ramirez A, Aguilera RJ (2019) A new pyridazinone exhibits potent cytotoxicity on human cancer cells via apoptosis and poly-ubiquitinated protein accumulation, Cell Biol Toxicol. https://doi.org/10.1007/s10565-019-09466-8
32. Sierra-Fonseca JA, Najera O, Martinez-Jurado J, Walker EM, Varela-Ramirez A, Khan AM, Miranda M, Lamango NS, Roychowdhury S (2014) Nerve growth factor induces neurite outgrowth of PC12 cells by promoting Gβγ-microtubule interaction. BMC Neurosci 15:132
33. Contreras L, Calderon RI, Varela-Ramirez A, Zhang H-Y, Quan Y, Das U, Dimmock JR, Skouta R, Aguilera RJ (2018) Induction of apoptosis via proteasome inhibition in leukemia/lymphoma cells by two potent piperidones, Cell Oncol. https://doi.org/10.1007/s13402-018-0397-1
34. Robles-Escajeda E, Lerma D, Nyakeriga AM, Ross JA, Kirken RA, Aguilera RJ, Varela-Ramirez A (2013) Searching in mother nature for anti-cancer activity: anti-proliferative and pro-apoptotic effect elicited by green barley on leukemia/lymphoma cells. PLoS ONE 8:e73508
35. Valdez B, Carr K, Norman J (2016) Violet-excited nim-DAPI allows efficient and reproducible cell cycle analysis on the Gallios

flow cytometer. Beckman Coulter Life Sciences. Houston, TX. http://www.bcilifesciences.com/flow/DAPIwhitepaper/BR-18940.pdf. Accessed Jan 2016
36. Varela-Ramirez A (2014) Female versus male cells in anti-cancer drug discovery: the winner is … AAPS Blog. https://aapsblog.aaps.org/2014/06/18/female-versus-male-cells-in-anti-cancer-drug-discovery-the-winner-is/. Accessed Sept 2018
37. Clayton JA, Collins FS (2014) Policy: NIH to balance sex in cell and animal studies. Nat News 509:282
38. García-Mata R, Bebök Z, Sorscher EJ, Sztul ES (1999) Characterization and dynamics of aggresome formation by a cytosolic Gfp-chimera. J Cell Biol 146:1239–1254
39. Lázaro-Diéguez F, Aguado C, Mato E, Sánchez-Ruíz Y, Esteban I, Alberch J, Knecht E, Egea G (2008) Dynamics of an F-actin aggresome generated by the actin-stabilizing toxin jasplakinolide. J Cell Sci 121:1415–1425
40. Leventis PA, Grinstein S (2010) The distribution and function of phosphatidylserine in cellular membranes. Ann Rev Biophys 39:407–427
41. Villanueva PJ, Martinez A, Baca ST, DeJesus RE, Larragoity M, Contreras L, Gutierrez DA, Varela-Ramirez A, Aguilera RJ (2018) Pyronaridine exerts potent cytotoxicity on human breast and hematological cancer cells through induction of apoptosis, PLoS ONE 13:e0206467
42. Pereira CS, Guedes JP, Gonçalves M, Loureiro L, Castro L, Gerós H, Rodrigues LR, Côrte-Real M (2016) Lactoferrin selectively triggers apoptosis in highly metastatic breast cancer cells through inhibition of plasmalemmal V-H+-ATPase. Oncotarget 7:62144
43. Zhang Y, Lima CF, Rodrigues LR (2014) Bovine lactoferrin induces cell cycle arrest and inhibits mTOR signaling in breast cancer cells. Nutr Cancer 66:1371–1385
44. Coleman ML, Sahai EA, Yeo M, Bosch M, Dewar A, Olson MF (2001) Membrane blebbing during apoptosis results from caspase-mediated activation of ROCK I. Nat Cell Biol 3:339
45. Fadeel B, Xue D (2009) The ins and outs of phospholipid asymmetry in the plasma membrane: roles in health and disease. Crit Rev Biochem Mol Biol 44:264–277
46. Savill J, Dransfield I, Gregory C, Haslett C (2002) A blast from the past: clearance of apoptotic cells regulates immune responses. Nat Rev Immunol 2:965
47. Guedes JP, Pereira CS, Rodrigues LR, Côrte-Real M (2018) Bovine milk lactoferrin selectively kills highly metastatic prostate cancer PC-3 and osteosarcoma MG-63 cells in vitro. Front Oncol. https://doi.org/10.3389/fonc.2018.00200
48. Sakahira H, Enari M, Nagata S (1998) Cleavage of CAD inhibitor in CAD activation and DNA degradation during apoptosis. Nature 391:96
49. Dolbeare F, Gratzner H, Pallavicini M, Gray J (1983) Flow cytometric measurement of total DNA content and incorporated bromodeoxyuridine. Proc Natl Acad Sci 80:5573–5577
50. Xiao Y, Monitto CL, Minhas KM, Sidransky D (2004) Lactoferrin down-regulates G1 cyclin-dependent kinases during growth arrest of head and neck cancer cells. Clin Cancer Res 10:8683–8686
51. Damiens E, El Yazidi I, Mazurier J, Duthille I, Spik G, Boilly-Marer Y (1999) Lactoferrin inhibits G1 cyclin-dependent kinases during growth arrest of human breast carcinoma cells. J Cell Biochem 74:486–498